

π^\pm Absorption and the Distribution of Neutrons in Nuclei

Morton M. Sternheim*

University of Massachusetts, Amherst, Massachusetts 01002

and

Elliot H. Auerbach†

Brookhaven National Laboratory, Upton, New York 11973

(Received 28 May 1971)

Optical-model calculations have been made of the sensitivity of the ratio of π^\pm absorption cross sections to the neutron-density distribution. Ratios accurate to a few tenths of 1% should be useful in determining neutron-density parameters.

I. INTRODUCTION

A recent reanalysis¹ of the old 700-MeV π^\pm -Pb inelastic scattering experiment of Abashian, Cool, and Cronin² led to a clear contradiction of then current suggestions of an appreciable neutron-rich surface or "halo" unless one introduced physically unreasonable neutron distributions. This report will present estimates of the sensitivity of similar experiments to nuclear-density parameters for representative nuclei as a function of energy.

The basic idea of such experiments is the following: Let us denote the total π^+ -proton cross section by $\sigma(\pi^+-p)$, the total π^+ -neutron cross section by $\sigma(\pi^+-n)$; similarly for $\sigma(\pi^- -p)$ and $\sigma(\pi^- -n)$. At energies for which $\lambda \equiv \sigma(\pi^+-n)/\sigma(\pi^+-p) = \sigma(\pi^- -p)/\sigma(\pi^- -n) > 2$, both π^\pm are strongly absorbed in the interior of a large nucleus, while in the surface region the π^+ are mainly absorbed by neutrons and the π^- by protons. The quantity

$$q \equiv \frac{\sigma(\pi^- -n)}{\sigma(\pi^+ -n)} - 1,$$

where the σ 's are π -nucleus "absorption" cross sections, is consequently sensitive to the properties of the surface region. (We include both inelastic scattering due to nucleon excitation and true absorption of pions in these cross sections.) In particular, q is sensitive to the relative densities of protons and neutrons. (A similar situation occurs for $\lambda \lesssim \frac{1}{2}$.) For example, changing R_n , the neutron half-density radius, by 10% changes the calculated value of q for Pb by about 0.05 at the most favorable energies. Figure 1 suggests $75 < T < 350$ MeV and $500 < T < 900$ MeV as promising pion kinetic energy regions for such experiments.

Because the π^\pm absorption ratio depends upon the relative densities of protons and neutrons, it complements data from electron scattering and muonic x-ray experiments. These electromagnetic probes

provide charge or proton distributions, but do not yield any information concerning neutron distributions.

Pion absorption may be compared with low-energy proton scattering, which has been used to measure neutron radii indirectly. Optical-model fits give an rms matter radius r_m . With a proton rms radius r_p from electromagnetic probes, the rms neutron radius is obtained from $Nr_n^2 = Ar_m^2 - Zr_p^2$. However, the difference $r_n - r_p$ obtained in this way is very sensitive to uncertainties in the r_p measurement, as well as to corrections to r_m arising from the finite range of the nucleon-nucleon force within nuclear matter. In the case of Pb^{208} , these considerations have led to a change in the reported value of $r_n - r_p$ from³ 0.5 ± 0.3 F to^{4,5} 0.13 ± 0.25 F.

The following sections will briefly describe the optical model used in our calculations to estimate the sensitivity of π^\pm absorption to the neutron distribution and the results obtained. Since, as discussed above, proton (charge) distributions are well determined by electron scattering and muonic x rays, we have not varied the proton parameters.

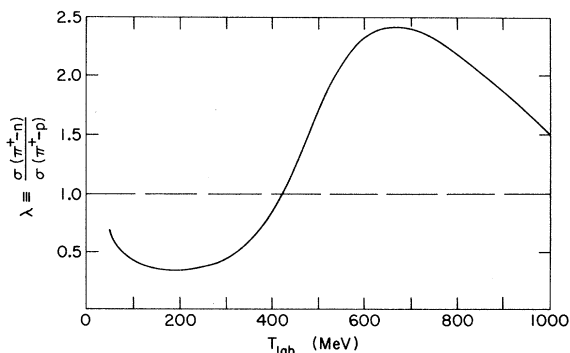


FIG. 1. The ratio of total π^+-p and π^+-n cross sections averaged over the motions of target nucleons within the nucleus. A Fermi-gas model with Fermi momentum 250 MeV/c is assumed.

II. OPTICAL MODEL

The calculations were performed using the ABACUS-M optical-model code⁶ which solves the partial-wave equations. A Coulomb potential plus an optical potential was used. Two optical potentials were tried, the velocity-dependent Kisslinger potential⁷ and the usual simple (velocity-independent) optical potential. The former contains a term which crudely takes into account the large p -wave amplitude in π - N scattering. It has been shown to predict correctly the general features of elastic scattering from about 25 to 100 MeV for several nuclei⁸ as well as the recent π^- -C data⁹ from 120 to 280 MeV.¹⁰ For π^+ , the original Kisslinger potential is

$$U = 2E_\pi V_{\text{opt}} = -Z[b_0 p_0^2 \rho_p(r) + b_1 \vec{p} \cdot \rho_p(r) \vec{p}] - N[b'_0 p_0^2 \rho_n(r) + b'_1 \vec{p} \cdot \rho_n(r) \vec{p}], \quad (1)$$

where the complex b_l terms are proportional to the forward-scattering amplitudes for π -nucleon scattering:

$$b_l = \frac{4\pi}{p_0^2} [f_l(0)]_{\text{lab}}^{\pi^+-p},$$

$$b'_l = \frac{4\pi}{p_0^2} [f_l(0)]_{\text{lab}}^{\pi^+-n} \quad (l=0, 1).$$

Here p_0 and E_π are the pion lab momentum and total energy, $\vec{p} = -i\vec{\nabla}$, and ρ_p and ρ_n are the target nucleus distributions of protons and neutrons, respectively, normalized to

$$\int \rho_p d^3x = \int \rho_n d^3x = 1. \quad (3)$$

Woods-Saxon densities were used, with

$$\rho_p(r) = \rho_{0p} [1 + e^{(r-R_p)/a_p}]^{-1}. \quad (4)$$

For $T \geq 300$ MeV, the π - N amplitude has signifi-

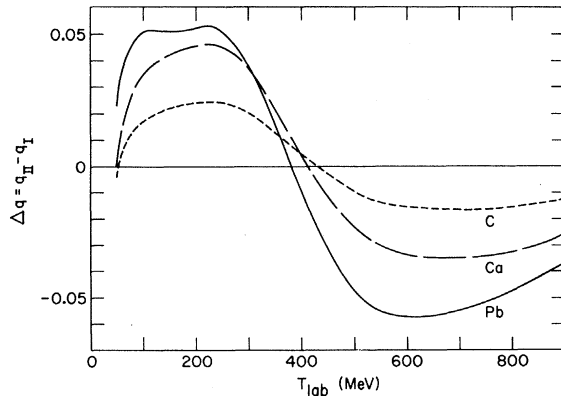


FIG. 2. The difference $\Delta q \equiv q(R_n = 1.1R_p) - q(R_n = R_p)$ for $a_n = a_p = 0.5$ F. (See Tables II-IV.) [$q \equiv \sigma(\pi^-A)/\sigma(\pi^+A) - 1$, where the σ 's are the reaction cross sections.]

cant $l > 1$ contributions. We have modified the Kisslinger model to also include these in the b_0 term of Eq. (1). For π^- , b_l and b'_l are interchanged.

The simple optical model is obtained with $b_0 = b_0 + b_1$, $b_1 = 0$ and similarly for b'_0, b'_1 . It does not fit the existing elastic scattering data from 25 to 280 MeV, but is expected to work well at somewhat higher energies. Its predictions for total cross sections are much smaller than those of the Kisslinger model for $T \leq 100$ MeV, but are within 5% of the Kisslinger energies for $T \geq 200$ MeV.

The calculations discussed below were done with both models. They are reported here only for the Kisslinger model, since for $T \geq 100$ MeV the dependence of total cross sections on nuclear parameters is essentially the same in both models.

The motion of the nucleons within the nucleus tends to slightly smooth out the optical parameters.¹¹ We assumed a Fermi-gas model with Fermi momentum 250 MeV/c. Figure 1 gives the ratio $\lambda \equiv \sigma(\pi^+n)/\sigma(\pi^+p)$ with this correction, and Table I gives the corrected parameters which were used in the calculations discussed in the next section.¹² The amplitudes $f_l(0)$ were calculated from the CERN phase shifts.¹³

III. CALCULATIONS

We computed absorption cross sections for C, Ca, and Pb from 50 to 900 MeV. These cross sections are tabulated in Tables II-IV for various values of ρ . The change in q resulting from increasing R_n from R_p to $1.1R_p$ with $a_p = a_n$ constant is plotted in Fig. 2, and increases from a maximum of 2.5% for C to 5.3% for Pb. The change in q resulting from varying a_n from 0.5 to 0.8 F - with the R_n adjusted to keep the rms neutron and

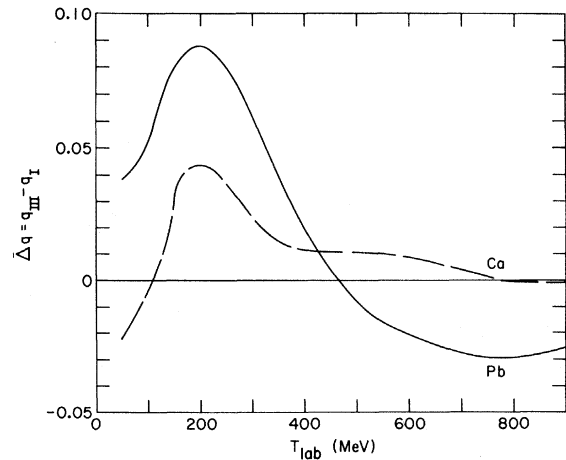


FIG. 3. The difference $\Delta q \equiv q(a_n = 0.8 \text{ F}) - q(a_n = 0.5 \text{ F})$, with equal proton and neutron rms radii in both cases. (See Tables III and IV.)

TABLE I. Pion-nucleus optical-model parameters. Averaged over Fermi gas with Fermi momentum 250 MeV/c. Units are F^3 . See discussion below Eqs. (1) and (2) for definitions.

T (MeV)	Reb_0	Imb_0	Reb_1	Imb_1	Reb'_0	Imb'_0	Reb'_1	Imb'_1
50	-6.02	0.53	14.39	2.37	3.78	0.89	3.80	0.99
100	-3.12	0.48	13.55	8.05	1.18	0.45	4.13	2.88
150	-2.04	0.45	5.91	12.39	0.57	0.31	1.76	4.15
200	-1.50	0.42	-1.12	9.63	0.41	0.25	-0.53	3.16
250	-1.16	0.39	-3.32	5.50	0.42	0.24	-1.16	1.82
300	-0.91	0.36	-3.05	2.89	0.49	0.25	-0.95	1.13
350	-0.72	0.34	-2.31	1.58	0.56	0.28	-0.68	0.86
400	-0.56	0.31	-1.68	0.91	0.63	0.35	-0.52	0.73
450	-0.44	0.29	-1.23	0.56	0.66	0.49	-0.45	0.62
500	-0.33	0.27	-0.90	0.37	0.65	0.63	-0.40	0.51
550	-0.24	0.27	-0.67	0.26	0.60	0.72	-0.36	0.42
600	-0.17	0.27	-0.50	0.20	0.54	0.78	-0.31	0.34
650	-0.10	0.29	-0.38	0.17	0.46	0.84	-0.27	0.27
700	-0.056	0.32	-0.29	0.15	0.36	0.89	-0.22	0.22
750	-0.022	0.34	-0.23	0.14	0.25	0.92	-0.17	0.19
800	-0.001	0.36	-0.18	0.13	0.14	0.90	-0.14	0.17
850	0.011	0.38	-0.15	0.13	0.047	0.85	-0.11	0.15
900	0.016	0.39	-0.12	0.12	-0.023	0.79	-0.081	0.14

TABLE II. Pion-carbon reaction cross sections: Case I: $R_n=R_p=2.06 F$, $a_n=a_p=0.5 F$; Case II: $R_n=1.1R_p=2.27 F$, $a_n=a_p=0.5 F$, $q \equiv (\sigma^-/\sigma^+ - 1)$.

T (MeV)	σ^+ (b)	Case I σ^- (b)	$q_I = \left(\frac{\sigma^-}{\sigma^+} - 1\right)$	σ^+ (b)	Case II σ^- (b)	q_{II}	$\Delta q = q_{II} - q_I$
50	0.3969	0.4689	0.1814	0.3972	0.4676	0.17724	-0.0042
100	0.4540	0.4851	0.0683	0.4597	0.4993	0.0861	0.0178
150	0.4271	0.4482	0.0494	0.4328	0.4640	0.0720	0.0226
200	0.3582	0.3738	0.0434	0.3632	0.3879	0.0680	0.0246
250	0.2842	0.2957	0.0406	0.2883	0.3072	0.0655	0.0249
300	0.2299	0.2386	0.0378	0.2336	0.2472	0.0586	0.0208
350	0.1992	0.2060	0.0342	0.2028	0.2124	0.0471	0.0129
400	0.1847	0.1902	0.0302	0.1885	0.1958	0.0344	0.0042
450	0.1813	0.1860	0.0260	0.1856	0.1897	0.0220	-0.0039
500	0.1841	0.1883	0.0223	0.1889	0.1912	0.0122	-0.0101
550	0.1878	0.1914	0.0195	0.1929	0.1940	0.0058	-0.0138
600	0.1923	0.1957	0.0174	0.1978	0.1981	0.0019	-0.0155
650	0.1997	0.2029	0.0157	0.2055	0.2054	-0.0006	-0.0163
700	0.2087	0.2116	0.0143	0.2149	0.2144	-0.0025	-0.0167
750	0.2159	0.2188	0.0132	0.2225	0.2217	-0.0034	-0.0167
800	0.2203	0.2230	0.0124	0.2270	0.2262	-0.0034	-0.0159
850	0.2225	0.2251	0.0118	0.2292	0.2285	-0.0028	-0.0146
900	0.2236	0.2261	0.0112	0.2301	0.2297	-0.0016	-0.0128

TABLE III. Pion-calcium reaction cross sections: Case I: $R_n = R_p = 3.76$ F, $a_n = a_p = 0.5$ F; Case II: $R_n = 1.1R_p = 4.14$ F, $a_n = a_p = 0.5$ F; Case III: $R_n = 2.33$ F, $R_p = 3.76$ F, $a_n = 0.8$ F, $a_p = 0.5$ F (rms proton and neutron radii both 3.45 F).

T (MeV)	Case I			Case II			Case III				
	σ^+ (b)	σ^- (b)	q_I	σ^+ (b)	σ^- (b)	q_{II}	σ^+ (b)	σ^- (b)	q_{III}	$q_{II} - q_I$	$q_{III} - q_I$
50	0.8682	1.154	0.3296	0.8851	1.178	0.3312	0.8245	1.077	0.3066	0.0016	-0.0230
100	0.9198	1.057	0.1487	0.9445	1.120	0.1854	0.9164	1.049	0.1448	0.0367	-0.0038
150	0.8642	0.9593	0.1099	0.8885	1.024	0.1528	0.8778	1.005	0.1446	0.0428	0.0347
200	0.7556	0.8270	0.0945	0.7774	0.8865	0.1403	0.7710	0.8782	0.1390	0.0458	0.0445
250	0.6391	0.6941	0.0859	0.6586	0.7455	0.1320	0.6494	0.7293	0.1230	0.0461	0.0371
300	0.5517	0.5949	0.0783	0.5705	0.6363	0.1154	0.5566	0.6133	0.1018	0.0371	0.0235
350	0.5017	0.5368	0.0699	0.5212	0.5686	0.0909	0.5029	0.5453	0.0844	0.0210	0.0145
400	0.4790	0.5084	0.0613	0.5003	0.5327	0.0647	0.4778	0.5125	0.0728	0.0033	0.0114
450	0.4765	0.5018	0.0530	0.5006	0.5208	0.0403	0.4739	0.5044	0.0644	-0.0127	0.0114
500	0.4852	0.5075	0.0460	0.5122	0.5232	0.0214	0.4820	0.5097	0.0574	-0.0246	0.0113
550	0.4947	0.5148	0.0407	0.5237	0.5287	0.0095	0.4914	0.5165	0.0511	-0.0312	0.0104
600	0.5054	0.5239	0.0365	0.5358	0.5372	0.0027	0.5024	0.5252	0.0455	-0.0338	0.0089
650	0.5210	0.5383	0.0332	0.5530	0.5521	-0.0016	0.5190	0.5397	0.0399	-0.0348	0.0067
700	0.5388	0.5553	0.0305	0.5725	0.5699	-0.0045	0.5383	0.5569	0.0346	-0.0045	0.0041
750	0.5529	0.5686	0.0284	0.5877	0.5843	-0.0058	0.5539	0.5706	0.0301	-0.0342	0.0017
800	0.5613	0.5763	0.0267	0.5964	0.5931	-0.0055	0.5634	0.5786	0.0269	-0.0322	0.0001
850	0.5657	0.5801	0.0253	0.6005	0.5981	-0.0040	0.5686	0.5825	0.0245	-0.0294	-0.0008
900	0.5681	0.5817	0.0241	0.6020	0.6010	-0.0017	0.5713	0.5843	0.0228	-0.0258	-0.0013

TABLE IV. Pion-lead reaction cross sections: Case I: $R_n = R_p = 6.52$ F, $a_n = a_p = 0.5$ F; Case II: $R_n = 1.1R_p = 7.17$ F, $a_n = a_p = 0.5$ F; Case III: $R_n = 5.79$ F, $R_p = 6.52$ F, $a_n = 0.8$ F, $a_p = 0.5$ F (rms proton and neutron radii both 5.38 F).

T (MeV)	Case I			Case II			Case III				
	σ^+	σ^-	$q_I = \left(\frac{\sigma^-}{\sigma^+} - 1\right)$	σ^+	σ^-	q_{II}	σ^+	σ^-	q_{III}	$q_{II} - q_I$	$q_{III} - q_I$
50	1.797	3.397	0.8897	1.923	3.680	0.9131	1.750	3.375	0.9282	0.0234	0.0384
100	1.934	2.798	0.4464	2.055	3.078	0.4977	1.974	2.963	0.5004	0.0513	0.0540
150	1.871	2.493	0.3326	1.990	2.753	0.3834	1.949	2.757	0.4141	0.0508	0.0815
200	1.719	2.201	0.2804	1.831	2.441	0.3331	1.800	2.464	0.3687	0.0527	0.0883
250	1.554	1.935	0.2452	1.660	2.154	0.2971	1.620	2.149	0.3269	0.0519	0.0817
300	1.445	1.744	0.2067	1.555	1.936	0.2453	1.495	1.898	0.2690	0.0385	0.0623
350	1.402	1.632	0.1641	1.522	1.796	0.1795	1.445	1.739	0.2038	0.0154	0.0397
400	1.403	1.574	0.1222	1.538	1.710	0.1123	1.444	1.650	0.1425	-0.0098	0.0203
450	1.431	1.555	0.0862	1.582	1.667	0.0538	1.478	1.611	0.0905	-0.0324	0.0043
500	1.468	1.559	0.0614	1.633	1.654	0.0132	1.523	1.604	0.0534	-0.0482	-0.0080
550	1.498	1.569	0.0473	1.670	1.656	-0.0086	1.559	1.608	0.0313	-0.0558	-0.0160
600	1.523	1.585	0.0404	1.699	1.670	-0.0174	1.590	1.621	0.0196	-0.0578	-0.0207
650	1.552	1.611	0.0376	1.731	1.698	-0.0195	1.625	1.647	0.0131	-0.0571	-0.0245
700	1.581	1.639	0.0366	1.764	1.731	-0.0186	1.663	1.678	0.0090	-0.0552	-0.0276
750	1.603	1.661	0.0364	1.786	1.758	-0.0160	1.691	1.703	0.0070	-0.0523	-0.0293
800	1.615	1.674	0.0366	1.797	1.776	-0.0117	1.706	1.719	0.0074	-0.0483	-0.0292
850	1.620	1.681	0.0374	1.800	1.789	-0.0060	1.712	1.729	0.0097	-0.0434	-0.0277
900	1.622	1.685	0.0387	1.799	1.800	0.0008	1.713	1.736	0.0135	-0.0379	-0.0252

proton radii equal – is shown in Fig. 3; it is as much as 8.8% for Pb.

IV. CONCLUSIONS AND COMMENTS

The ratio of π^+/π^- absorption cross sections is sensitive to details of the neutron density, assuming the proton density is known already, e.g., from electron scattering. It provides a useful constraint on the neutron distribution – one which contains information about the nuclear surface, although it does not fix uniquely a particular moment or parameter. An accuracy of a few tenths of a percent in the ratio is required for interesting results. The validity of the optical model used can

be verified by studying the energy dependence of the cross sections¹ and of the ratios,² and is itself an interesting question worth further study. Note that the ratios are quite insensitive to the optical parameters used.¹

Differential elastic π^\pm scattering data will also be quite sensitive to details of the nucleon densities, particularly at large momentum transfers.¹ This will be explored in a later paper.

ACKNOWLEDGMENT

One of us (MMS) would like to thank Los Alamos Scientific Laboratory for its hospitality. J. Silver and A. Lopez assisted with the computations.

*Research supported in part by the National Science Foundation. Part of this work was done while the author was a Visiting Staff Member at Los Alamos Scientific Laboratory.

†Work performed under the auspices of the U. S. Atomic Energy Commission.

¹E. H. Auerbach, H. M. Qureshi, and M. M. Sternheim, Phys. Rev. Letters **21**, 162 (1968).

²A. Abashian, R. Cool, and J. W. Cronin, Phys. Rev. **104**, 855 (1956).

³G. W. Greenlees, G. J. Pyle, and Y. C. Tang, Phys. Rev. Letters **17**, 33 (1966); Phys. Rev. **171**, 1115 (1968).

⁴G. W. Greenlees, W. Makofske, and G. J. Pyle, Phys. Rev. C **1**, 1145 (1970).

⁵D. Slanina and H. McManus, Nucl. Phys. **A116**, 271 (1968).

⁶E. H. Auerbach and M. M. Sternheim, Brookhaven National Laboratory Report No. BNL-12696, 1968 (unpublished).

⁷L. S. Kisslinger, Phys. Rev. **98**, 761 (1955).

⁸E. H. Auerbach, D. M. Fleming, and M. M. Sternheim, Phys. Rev. **162**, 1683 (1967); **171**, 1781 (1968).

⁹F. Binon *et al.*, Nucl. Phys. **B17**, 168 (1970).

¹⁰M. M. Sternheim and E. H. Auerbach, Phys. Rev. Letters **25**, 1500 (1970).

¹¹M. Crozon *et al.*, Nucl. Phys. **64**, 567 (1965).

¹²The units for b used in the table and in the ABACUS-M code are F^3 . Thus in Eq. (3) σ is expressed in F^2 and p in F^{-1} .

¹³A. Donnachie, R. G. Kirsopp, and C. Lovelace, Phys. Letters **26B**, 161 (1968); see also CERN Report No. TH-838, addendum (to be published).

High-Spin Proton States Observed in the Reactions $^{90}\text{Zr}(\alpha, t)^{91}\text{Nb}$ and $^{92}\text{Mo}(\alpha, t)^{93}\text{Tc}$ at 50 MeV*

M. S. Zisman and B. G. Harvey

Lawrence Berkeley Laboratory, University of California, Berkeley, California 94720

(Received 16 April 1971)

The reactions $^{90}\text{Zr}(\alpha, t)^{91}\text{Nb}$ and $^{92}\text{Mo}(\alpha, t)^{93}\text{Tc}$ have been investigated with a 50-MeV α -particle beam from the Berkeley 88-in. cyclotron. Comparisons are made with the results of ($^6\text{He}, d$) experiments on the same targets in order to locate high-spin ($l > 2$) levels in ^{91}Nb and ^{93}Tc . The $^{91}\text{Nb}(4.18 \text{ MeV})$ and $^{93}\text{Tc}(3.91 \text{ MeV})$ levels are probable $l=4$ or 5 levels, in contrast to the ($^6\text{He}, d$) results. A difference in Q values for the reactions $^{90}\text{Zr}(\alpha, t)^{91}\text{Nb}$ and $^{91}\text{Zr}(\alpha, t)^{92}\text{Nb}$ of $680 \pm 25 \text{ keV}$ yields a Q value for the reaction $^{90}\text{Zr}(\alpha, t)^{91}\text{Nb}$ of $-14.643 \pm 0.027 \text{ MeV}$, which is not consistent with the presently accepted mass excess of $-86.750 \pm 0.06 \text{ MeV}$ for ^{91}Nb .

I. INTRODUCTION

In recent years there have been many studies¹⁻⁶ of proton configurations in the $N=50$ nuclei

^{91}Nb and ^{93}Tc . The locations of these proton states are of interest for comparison with shell-model calculations^{7,8} and the centroid positions are useful in predicting energies of two-particle proton-